

DISCOVERY OF THE 11.2 MICRON POLYCYCLIC AROMATIC HYDROCARBON BAND IN ABSORPTION TOWARD MONOCEROS R2 IRS 3

JESSE D. BREGMAN

Astrophysics Branch, NASA Ames Research Center, MS 245-6, Moffett Field, CA 94035

THOMAS L. HAYWARD

Gemini Observatory, 670 North A'ohoku Place, Hilo, HI 96720

AND

G. C. SLOAN

Institute for Scientific Research, Boston College, Chestnut Hill, MA 02467

Received 2000 July 28; accepted 2000 September 22; published 2000 November 9

ABSTRACT

Interpretation of the infrared emission bands is difficult because these bands likely arise from a mixture of ionized and neutral polycyclic aromatic hydrocarbon (PAH) molecules. Modeling the emission process is also difficult because the size distribution of the molecules, their ionization state and excitation, and the geometry of the emitting regions are generally unknown. If these molecular bands could be found in absorption, many of these factors would be eliminated, making it much easier to interpret the data. We have discovered an absorption band in Monoceros R2 IRS 3 centered at 11.25 μm that we identify with a C–H out-of-plane vibrational mode of PAH molecules. The shape and position of the band are very similar to that seen in emission in planetary nebulae, H II regions, and the interstellar medium.

Subject headings: infrared: ISM: lines and bands — ISM: molecules — stars: individual (Monoceros R2 IRS 3)

1. INTRODUCTION

The infrared emission features (IEFs, also known as the unidentified infrared [UIR] bands) are observed in a wide variety of sources, including planetary nebulae, H II regions, photo-dissociation regions, proto–planetary nebulae, and starburst galaxies, and in the diffuse interstellar medium of our own Galaxy. There is much evidence that they arise from the UV and visible light excitation of large aromatic molecules, particularly polycyclic aromatic hydrocarbons (PAHs), which contain about 10% of all the interstellar carbon (Allamandola, Tielens, & Barker 1989). With such large abundances, one would expect to observe these bands in absorption toward regions with high extinction. However, these bands are not easy to observe since other grain constituents such as H₂O and silicates have strong absorption bands that overlap the PAH bands.

The strongest IEFs occur at 3.3, 6.2, 7.7, 8.6, and 11.2 μm , with broad plateaus extending from 6 to 9 and 11 to 14 μm . In PAHs, which are multiringed carbon-based molecules with hydrogen atoms on the periphery, the 3.3 μm band is due to the C–H stretching mode, the 6.2 and 7.7 μm bands are due to C–C modes, and the 8.6 and 11.2 μm bands are due to C–H in-plane and out-of-plane bending modes, respectively. The vibration frequency of the out-of-plane bending mode depends on the arrangement of peripheral hydrogen atoms, so that the feature occurs at progressively longer wavelengths as the number of adjacent hydrogens increases from one (solo) to four (quattro) (see Cohen, Tielens, & Allamandola 1985, Fig. 3).

In the molecular cloud surrounding Monoceros R2 IRS 3, Sellgren, Smith, & Brooke (1994) reported a tentative measurement of an absorption band at 3.25 μm with a 5% strength that they subsequently confirmed and identified as the C–H stretch in PAH molecules (Sellgren et al. 1995). Then, Brooke, Sellgren, & Smith (1996) observed the same band toward the embedded protostars S140 IRS 1 and NGC 7538 IRS 1. If the identification with PAHs were correct, then we would expect other PAH bands to be present in absorption. Schutte et al. (1998) report a possible detection of the 6.2 μm PAH band in absorption toward bright

background sources in the direction of the Galactic center. However, they did not detect any other PAH absorptions in these objects that would confirm the identification. At 11.2 μm , where we would expect the solo out-of-plane PAH band, no observations have been published that have a sufficient signal-to-noise ratio or spectral resolution to see a weak PAH absorption feature. The *Infrared Space Observatory (ISO)* short-wave spectrometer data should have provided these data, but an unfortunate calibration problem at 11.1 μm produced an emission feature (5% high, 0.1 μm wide) accompanied by a broad absorption feature that was a few percent deep, extending from 10.8 to 11.2 μm and precluding the detection of weak absorption features throughout this wavelength range.

One of the major difficulties of identifying the infrared emission bands with a particular PAH molecule is that the emission arises from a family of molecules rather than from an individual species. Emission at short wavelengths is dominated by small molecules, while at long wavelengths it is dominated by large molecules, complicating the identification and analysis of the emission spectra (Schutte, Tielens, & Allamandola 1993). Thus, the emission at 3.3 μm is dominated by a different mix of molecules than those that produce the 11.2 μm band, even though both involve vibrations of C–H bonds. To complicate matters further, the molecular mix includes both neutral and ionic species. In absorption, the same mixture of molecules contributes to all vibrational modes, potentially simplifying comparisons with laboratory data. Also, absorption strengths measured in the laboratory are directly applicable to interstellar absorption bands without the need to model an emission spectrum of an unknown mixture of ionized and neutral PAHs.

In this Letter, we report the first measurement of the out-of-plane absorption from PAHs at 11.2 μm toward Mon R2 IRS 3, confirming the identification of the 3.25 μm band by Sellgren et al. (1994, 1995) as being due to absorption by PAHs. In § 2 we describe the observations and data analysis, and in § 3 we discuss the results.

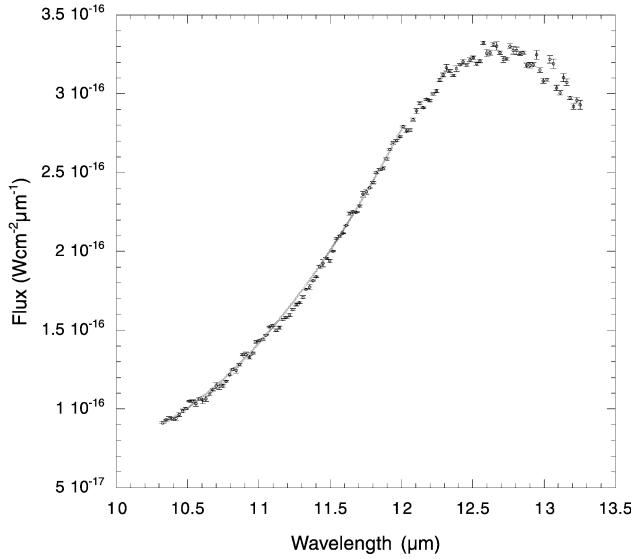


FIG. 1.—Spectrum of Mon R2 IRS 2 shown with a second-order polynomial (solid gray line) fitted to the data points from 10.3 to 12.2 μ m, excluding those points from 11.1 to 11.6 μ m.

2. OBSERVATIONS AND DATA ANALYSIS

SpectroCam-10 (Hayward et al. 1993) observations of Mon R2 IRS 3, using a 1"-wide slit that is 16" long with 0.25 square pixels, were made from the 5 m Hale telescope at the Palomar Observatory.¹ We used the low-resolution grating and a 128×64 section of a 128×128 pixel Si : As array with 128 detectors in the spectral direction. This combination provides wavelength coverage from 10.3 to 13.3 μ m at a spectral resolution of 100. The standard star α Tauri was observed at a similar air mass, thus providing a good air-mass correction. All observations were made using a standard chop-and-nod sequence.

To process the data, a set of either 8, 16, or 32 spectra were added together and then flat-fielded. Spectra were extracted by adding together the brightest three rows of the α Tau spectrum, corresponding to the FWHM of the stellar image. The same procedure was followed for Mon R2 IRS 3. The Mon R2 and α Tau spectra were spectrally aligned by matching terrestrial absorption lines. The Mon R2 data were then divided by α Tau and multiplied by the α Tau spectrum taken from Walker & Cohen (1992). Since Mon R2 and α Tau were not observed at the same grating tilt, the division left a residual oscillation that was due to fringing in the detector. To avoid introducing extraneous features into the data, the fringing was removed as the last step of data processing.

Figure 1 shows the results of the data processing. The smoothly increasing continuum from short to long wavelengths is due to the long-wavelength wing of the 10 μ m silicate absorption feature. In order to look for PAH absorption features, we fitted a second-order polynomial to all the data points in the spectrum from 10.3 to 12.2 μ m, with the long-wavelength cutoff determined by the inflection of the data. There was an obvious absorption in the 11.2 μ m region relative to the adjacent continuum. However, since we included the absorption feature in the polynomial fit, the continuum near 11.2 μ m was above the polynomial. To better fit only the continuum, we defined it by

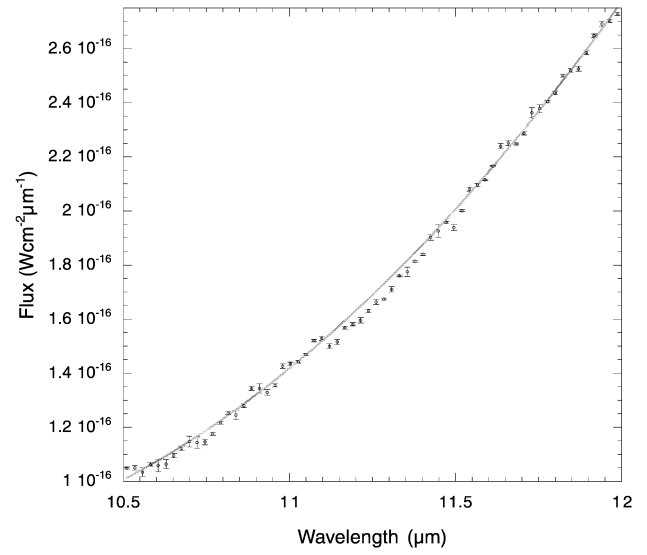


FIG. 2.—Same as Fig. 1, except that only the region between 10.5 and 12.0 μ m is shown. The depression in the data between 11.1 and 11.5 μ m, below the smooth fit, is clearly visible.

sections of spectra from 10.3 to 11.1 μ m and from 11.5 to 12.2 μ m, which excluded the majority of the 11.2 μ m absorption. This fit, a second-order polynomial, appears as a solid gray line in Figure 1. The data points from 11.1 to 11.6 μ m lie below the polynomial, as shown clearly in Figure 2. The Mon R2 spectrum was then divided by the polynomial in order to remove the smooth continuum, leaving a residual spectrum normalized to 1 (Fig. 3). This spectrum has had the detector fringing removed with a fast Fourier transform filter centered on the oscillation frequency. Also shown in the figure is an inverted and scaled spectrum of the 11.2 μ m feature in BD +30°3639, a bright planetary nebula with strong PAH emission (Witteborn et al. 1989). The Mon R2 spectrum shows an absorption with a sharp cut-on just longward of 11.1 μ m that is a good match to the short-wavelength side of the BD +30°3639 spectrum. Witteborn et al. (1989) show that the 11.2 μ m feature position and shape

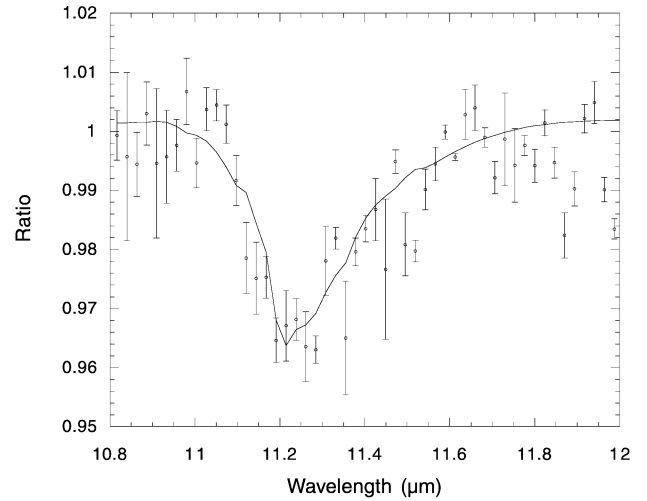


FIG. 3.—Mon R2 flux divided by the smooth polynomial fit shown in Figs. 1 and 2, showing the shape of the absorption centered at 11.2 μ m. For comparison, an inverted and scaled spectrum of the planetary nebula BD +30°3639 (Witteborn et al. 1989) is shown as a solid line.

¹ Observations at the Palomar Observatory were made as part of a continuing collaborative agreement between the California Institute of Technology, Cornell University, and the Jet Propulsion Laboratory.

are fairly constant among a variety of objects and that the BD +30°3639 spectrum is not unique. We used BD +30°3639 for this comparison because we had the spectrum available in a convenient format. We also tried a fourth-order polynomial that was fitted to all the Mon R2 data in order to look for longer wavelength absorption features, but due to the combination of increased background noise and atmospheric absorptions, we failed to find any additional statistically significant features. Features with absorption depths less than 2% would not have been undetected.

3. DISCUSSION

We base the identification of this 11.2 μm absorption feature with PAHs on three facts. First, there is another PAH band in absorption at 3.25 μm observed by Sellgren et al. (1994, 1995). Second, the wavelength agrees quite well with the emission observed in other objects thought to be due to PAHs, and third, it has an integrated absorption strength relative to the strength of the 3.25 μm band that is consistent with laboratory data of PAHs.

The integrated absorption strength for both the 3.25 and 11.2 μm bands is just the product of the optical depth τ and the FWHM of the band in frequency units $\Delta\nu$. Using triangular approximations for the shape of both bands gives the results shown in Table 1.

Laboratory studies of absorption by neutral PAHs isolated in an argon matrix (Hudgins & Sandford 1998a, 1998b, 1998c) show that for molecules that contain solo hydrogens (such as anthracene, tetracene, and pentacene), the intrinsic band strength of the C–H stretch (near 3.3 μm) is generally about half that of the C–H out-of-plane solo bending mode (near 11.2 μm) per C–H bond. We have chosen to use the relative band strengths for neutral, gas-phase PAHs for several reasons. PAH cations are unlikely in the low-UV environment near the protostar, and since the intrinsic intensities of the C–H stretch in PAH cations is an order of magnitude less than in neutral PAHs (Szczerpanski & Vala 1993), 100% of the total available carbon would have to be tied up in PAHs to produce the observed 3.25 μm band. Also, in both PAH cations and solid-state PAHs (Joblin et al. 1994), the relative strengths of the C–H stretch and C–H bend would imply that only 4% of the C–H bonds are solo hydrogens. We would then expect strong duo and trio bands, which are not observed. Using the intrinsic band intensities for neutral isolated PAHs and the observed ratio of the C–H solo bend to stretch of 0.24, only one-eighth of the C–H bonds in the PAH mixture can be solo hydrogens.

The apparent strength of the C–H stretch relative to the C–H out-of-plane solo mode bend can be explained by examining laboratory spectra for a sample of PAHs (Hudgins & Sandford 1998a, 1998b). The laboratory data show that while there is a large variation of the wavelength of the C–H out-of-plane band, leading to many weak absorptions throughout this wavelength region that might be impossible to detect individually, the C–H stretches for all of these PAHs occur within the FWHM of the absorption bands observed in absorption by Sellgren et al. (1995) and Brooke et al. (1996). Thus, given a mixture of PAHs, the C–H stretch absorptions will overlap, and the combined feature should be significantly stronger than any single C–H bend absorption.

In PAH emission sources, the wavelength region of the out-of-plane bend shows narrow features at 11.2, 11.8, and 12.7 μm and a broad plateau extending from 11 to 13 μm that is usually attributed to overlapping emission from the out-of-

TABLE 1
BAND STRENGTHS

Wavelength (μm)	τ	$\Delta\nu$	$\tau\Delta\nu$	Ratio to 3.25
3.25 ^a	0.045	75	3.37	...
11.3	0.037	22	0.81	0.24
Duo/trio modes	<0.02	

^a Data from Sellgren et al. 1995.

plane bending modes in a mixture of PAHs (Cohen et al. 1985; Witteborn et al. 1989). In the planetary nebula BD +30°3639, the ratio of energy in the 11.2 μm band to the total energy (11.2 μm band + plateau) is $\frac{1}{3}$, while in two H II and photo-dissociation regions from the *ISO* database (IRAS 03035+5819 and IRAS 18416–0420), the ratio is $\frac{1}{6}$. Given that the intrinsic band strength of the out-of-plane solo mode is about twice that of the other out-of-plane modes (D. M. Hudgins 2000, private communication), the proportion of solo hydrogen bonds in interstellar PAHs producing the sharp 11.2 μm band is between 9% and 20%, in agreement with our result for Mon R2 of 12%. Thus, it appears that the strength of the 11.2 μm absorption band in Mon R2 relative to the 3.25 μm absorption is consistent with the proportion of solo hydrogen bonds observed in the interstellar medium in emission. However, a substantial portion (about 30%) of the plateau shortward of about 11.6 μm must also be due to solo hydrogens. In H II regions, the energy in the plateau attributable to solo modes can exceed the energy in the 11.2 μm band by 50%. Including the energy from the plateau changes the proportion of solo hydrogen bonds to between 25% and 33% of the total out-of-plane emission. Since the plateau is rather broad and is only about half the amplitude of the sharp feature, if it were present in Mon R2, we would be unable to distinguish it from the continuum. Thus, we interpret the apparent strength of the solo hydrogen mode as being due just to its intrinsic band strength rather than any mechanism that favors a large fraction of solo hydrogens.

The proportion of C–H bonds in the solo mode (less than or about equal to 30%) has implications for which PAHs could be present around Mon R2. Long linear PAHs cannot dominate the mixture since only the smallest molecules (anthracene, $\text{C}_{14}\text{H}_{10}$, solo/total = 0.20, and tetracene, $\text{C}_{18}\text{H}_{12}$, solo/total = 0.33) have sufficiently low ratios of solo/total C–H bonds. Large condensed PAHs have the same problem for molecules larger than circumcoronene ($\text{C}_{42}\text{H}_{16}$, solo/total = 0.25) since only solo hydrogens are added as the molecules get larger. A few of the PAHs expected in the interstellar medium have no solo hydrogens (e.g., coronene and hexabenzocoronene), and such molecules added to the mix will lower the solo/total ratio. Thus, it appears that the PAH mixture, consistent with the observed proportion of solo hydrogen bonds, is dominated by moderately sized condensed molecules.

The similarity of the shape of the absorption band in Mon R2 to that of the emission band in BD +30°3639 is striking. Within the uncertainties, nearly all the data from 11.1 to 11.6 μm fall on the scaled BD +30°3639 spectrum. This agreement suggests that the PAH mixture producing the absorption in Mon R2 is similar to the PAH mixture giving rise to the emission features. Since Bernstein et al. (1999) show that PAHs frozen into a water matrix in molecular clouds are rapidly processed in a way that produces large numbers of solo hydrogens, our data suggest that the PAHs are not contained within the water ice matrix. We conclude that the life cycle of a PAH likely proceeds as follows. PAHs are created in outflows

from carbon stars, along with other carbon-based molecules, and appear in emission in proto-planetary nebulae as a complex mix that includes aromatic and aliphatic components. This molecular mix not only produces an 11.2 μ m band but also bands of comparable strength at 12.1 and 12.4 μ m (Kwok, Volk, & Hrivnak 1999). Processing by UV during the planetary nebula phase modifies the PAH mixture, resulting in a spectrum dominated by the 11.2 μ m feature with much weaker duo and trio bands at 11.8 and 12.7 μ m. Further UV processing occurs while

the molecules are in the interstellar medium, as indicated by changes to the 7.7 μ m band and the relative strengths of the 11.2 μ m feature and underlying plateau, but the shape of the 11.2 μ m feature remains unchanged. Only the most stable and largest molecules survive, and it is this mix of PAH molecules that we observe in absorption in Mon R2.

We are grateful to the staff of the Palomar Observatory for their excellent support that made these observations possible.

REFERENCES

- Allamandola, L. J., Tielens, A. G. G. M., & Barker, J. R. 1989, *ApJS*, 71, 733
 Bernstein, M. P., Sandford, S. A., Allamandola, L. J., Gillette, J. S., Clemett, S. J., & Zare, R. N. 1999, *Science*, 283, 1135
 Brooke, T. Y., Sellgren, K., & Smith, R. G. 1996, *ApJ*, 459, 209
 Cohen, M., Tielens, A. G. G. M., & Allamandola, L. J. 1985, *ApJ*, 299, L93
 Hayward, T. L., Miles, J. E., Houck, J. R., Gull, G. E., & Shoenwald, J. 1993, *Proc. SPIE*, 1946, 334
 Hudgins, D. M., & Sandford, S. A. 1998a, *J. Phys. Chem.*, 102, 329
 ———. 1998b, *J. Phys. Chem.*, 102, 344
 ———. 1998c, *J. Phys. Chem.*, 102, 353
 Joblin, C., d'Hendecourt, L., Leger, A., & Defourneau, D. 1994, *A&A*, 281, 923
 Kwok, S., Volk, K., & Hrivnak, B. J. 1999, *A&A*, 350, L35
 Schutte, W. A., Tielens, A. G. G. M., & Allamandola, L. J. 1993, *ApJ*, 415, 397
 Schutte, W. A., et al. 1998, *A&A*, 337, 261
 Sellgren, K., Brooke, T. Y., Smith, R. G., & Geballe, T. R. 1995, *ApJ*, 449, L69
 Sellgren, K., Smith, R. G., & Brooke, T. Y. 1994, *ApJ*, 433, 179
 Szczepanski, J., & Vala, M. 1993, *ApJ*, 414, 646
 Walker, R. G., & Cohen, M. 1992, *An Atlas of Selected Calibrated Stellar Spectra* (NASA-CR 177604; Moffett Field: NASA/ARC)
 Witteborn, F. C., Sandford, S. A., Bregman, J. D., Allamandola, L. J., Cohen, M., Wooden, D. H., & Graps, A. L. 1989, *ApJ*, 341, 270